PROGRESS IN COLOR, COLORANTS AND COATINGS

available online @ www.pccc.icrc.ac.ir

Prog. Color Colorants Coat. 9 (2016), 1-16

Ministry of Science, Research and Technology
Institute for Color Science and Technology

Synthesis, Characterization and Application of Silica Aerogel-Eggshell Nanocomposite for the Dye Removal from Colored Wastewater

M. Madadi[1], F. Tadayon[1] and M. E. Olya[2*]

[1] Department of Chemistry, North Tehran Campus, Islamic Azad University, P. O. Box: 19585-936, Tehran, Iran.

[2] Department of Environmental Research, Institute for Color Science and Technology, P. O. Box: 16765-654, Tehran, Iran.

ARTICLE INFO

Article history:
Received: 4 May 2015
Final Revised: 18 Aug 2015
Accepted: 1 Dec 2015
Available online: 1 Dec 2015

Keywords:
Basic Violet 16
Eggshell
Nanocomposite
Silica Aerogel

ABSTRACT

In the current study, silica aerogel-eggshell was synthesized and characterized as nano-adsorbent for dye removal from colored wastewater. The nanocomposite structure was characterized by Fourier transform infrared spectra and scanning electron microscope. The ability of adsorption silica aerogels-egg shell nanocomposite for removal of basic violet 16 dye from aqueous solutions was studied using batch adsorption system and compared with two other adsorbents such as egg shell and silica aerogels. The results showed that adsorption power of basic violet 16 dye increased by silica aerogels-egg shell nanocomposite. The adsorbents were evaluated for removal of dye under different pH values, temperatures, adsorbent dosages and contact times. The optimum pH for dye removal by nanocomposite was 8, while the optimum pH for the two other adsorbents of basic violet 16 was about 12. The optimum temperature and adsorbent dosage for dye removal was 35°C and 5g/L, respectively. Eventually, the equilibrium was achieved for the dye removal after 90 min of contact time. In order to better understand the adsorption process, the experimental data were analyzed with Langmuir and Freundlich isotherm models and it was discerned that synthesized adsorbents were well fitted by Freundlich equation. *Prog. Color Colorants Coat. 9 (2016), 1-16*

1. Introduction

Water pollution as a result of dyeing industry effluents is a reason for serious concern because the dyes undergo chemical changes and may be more toxic and carcinogenic under environmental conditions. Today,more than ten thousand dyes are produced annually which can be of many different structural varieties [1]. A wide variety of organic pollutants introduced into the natural water are caused by different sources such as textile industries, paper and pulp industries, dye and dye intermediates industries, pharmaceutical industries, tannery, and Kraft bleaching industries [2]. Of the main sources with severe

*Corresponding author: olya-me@icrc.ac.ir

pollution problems are the textile industry and its dye-containing wastewaters [3]. Approximately 10-25% of textile dyes are lost during the dyeing process, and 2-20% is discharged as effluent in the environment. There are several different kinds of dyes, such as reactive azo dye, metal complex, and cationic and anionic dyes [4]. Basic Violet 16 (BV 16) is a cationic dye, highly water soluble and nonvolatile which is widely used in textile, bullpen, preparing carbon paper, leather industries, stamp pad inks and paints. However, it should be eliminated from industrial wastewaters due to its damages on skin, eyes, and gastrointestinal, respiratory tract [5]. The methods used to remove compound dyes are chemical precipitation [6], ion-exchange mechanism [7], and reverse osmosis [8], electro chemical reduction membrane processes [9] and adsorption technique [10]. The adsorption process is an effective method applied in industries for removal pollution [11]. Different materials have been used to remove dyes from waste waters such as bioflocculants [12], bone powder [13], rice hull ash [14], activated carbon [15], and silica gel [16]. Nowadays new adsorbents with high specific surface areas, high adsorption capacity and economic materials are still needed. Pore size, pore distribution and surface areas are the key factors in the adsorption process [17]. Silica aerogels convene all these conditions as they are extremely porous and consisted of more than 96 percent air [18]. An aerogel is synthesized by the “sol-gel process”. During this process, organic compounds containing silica undergo a chemical reaction producing silicon oxide $(SiO_2)_2$ [19]. Finally, gel is dried by ambient pressure drying technique so that the solvent is extracted from the gel body leaving the silicon oxide network filled with air [20].

The large surface areas and great pore volumes of eggshell enable it to adsorb efficiently many kinds of pollutants [21]. Despite this, eggshell does not have appropriate functional groups for adsorbing dye compounds frugally [22]. To overcome this limitation, many methods have been introduced for modifying the eggshell surface using chemical/physical treatment [23].

In the current study, we have prepared a novel nanocomposite of silica aerogel-eggshell with sol-gel process at ambient pressure drying method [24]. The adsorbent structure was characterized by Fourier transform infrared spectrum (FT-IR) and scanning electron microscopy (SEM). In this research, a new adsorbent was synthesized by combining two separate adsorbents and used for the removal of Basic BV16 dye from aqueous solutions. Adsorption isotherms on the adsorption of BV16 were evaluated in a batch system. The effects of the BV16 ions concentration, pH, temperature and adsorbent dosage were also studied to determine the optimal adsorption conditions.

2. Experimental

2.1. Materials and Methodes

The reagents applied in the present study were of analytical grade, obtained from Merck. Tetraethylorthosilicate (TEOS), Trimethoxy-methylsilane (TMMS), Ethanol 25 wt. % and NH4F used in this study were obtained from Merck. Deionized water of high purity (from a Millipore ultrapure water system) was exploited as well. Basic Violet 16 (BV16) dye was obtained from Alvan Sabet Co. (Hamedan, Iran) and used without additional purification. Acetic acid and sodium hydroxide were used for pH adjustment (4-13). The dye concentration of the BV16 ion solutions was determined by double Agilent spectrophotometer (Cary 100 Bio, Technologies). The chemical structure of this cationic dye is presented in Table 1. The pH of the solution was measured by a Honba-F12.

Table 1: The chemical properties of BV16.

Chemical formula	$C_{23}H_{29}CLN_2$
Molecular mass (g.mol^{-1})	368.5
C.I. number	6359-45-1
Water solubility(20°C)	high
λ_{max}(nm)	544

2.2. Preparation of adsorbent

2.2.1. Preparation of eggshell

The egg shells were gathered from a candy store, carefully washed and rinsed with distilled water for the preparation of the egg shell [25]. It was dried at 80°C for 10 h. The dried shells were ground by ball mill and passed through what man cellulose filter papers. The required particle size was <0.450 µm.

2.2.2. Preparation of nanocomposite

The silica gel-eggshell nanocomposite was synthesized by mixing TEOS, TMMS, Ethanol, NH_4F [26] and egg shell. In order to get the best aerogels in terms of low density and high hydrophobicity, the molar ratio of TEOS: TMMS: Ethanol: NH_4F was 1:0.31:33:3.6, respectively. Silica wet gel was prepared with TEOS as the starting material. The TEOS was diluted with Ethanol and then TMMS and NH_4F solution were added to the mixture by stirring at 1500 rpm for 30 min. After wards, the eggshell was added to the blend using a homogenizer. After gelation, the gel was left for 24h. The hydrogel was immersed into Ethanol and remained for 5 days at room temperature in order to strengthen its network. Finally, the wet gels were dried at 40°C, 60°C, 80°C, 100°C, 150°C and 200°C in an oven. To protect gel from temperature shock and shrinkage, temperature was increased slowly until the desired temperature was reached [24].

2.3. Adsorbent characterization

The textural properties of the samples were studied by infrared spectroscopy measurements (FT-IR, Perkin-Elmer, spectrum 100). The surface area and porosity of the prepared adsorbents were observed with scanning electron microscopy (SEM-EDX, XL30 and Philips Nederland).

2.4. Adsorption experiments

The adsorption of BV16 dye by three adsorbents including silica aerogel, eggshell and silica aerogel-eggshell nanocomposite was studied by the batch technique. The batch method adsorption was selected due to its simplicity. The pH of the dye solution was adjusted to 4.0-13.0 using a buffer. The mixing time was 3h and all experiments were done at room temperature. After reaching equilibrium, the suspensions were centrifuged at 3000 rpm for 20min. Finally, the solution was collected and analyzed dye concentration by UV-Vis spectrometry. The influence of several parameters such as contact time, pH, the amount of adsorbent and temperature on the adsorption process was also studied. The results of these studies were used to find the optimum adsorption capacity measurements.

The percentage of dye adsorbed on the adsorbent was calculated using Eq. (1).

$$E\,(\%) = (C_0 - C_e) \times 100 / C_0 \qquad (1)$$

Where E is dye ion removal in %, C_0 initial dye concentration and Ce equilibrium concentration of test solution.

The amount of BV16 dye adsorbed on the three adsorbents at equilibrium was obtained using the following equation:

$$q_e = \frac{(C_0 - C_e)_v}{w} \qquad (2)$$

where q_e is the amount of dye adsorbed at equilibrium ($mol.g^{-1}$), V is the volume of the solution (L), m is the mass of the adsorbent (g), C_0 and Ce are the initial and equilibrium concentrations of the dye, respectively, computed from the calibration curve. Adsorption isotherms were considered by mixing 0.1 g of adsorbents in the flasks containing 20 mL of different initial BV16 dye ion concentrations for 3 h. The initial pH was adjusted to 12.0 and 8.0 for BV16 dye ions. Two isotherm equations have been investigated in the current study: Freundlich and Langmuir.

3. Results and discussion

3.1. Properties of nanocomposite silica aerogel-eggshell

3.1.1. The Microstructure of the adsorbents

The morphology of the three adsorbents was examined by scanning electron microscope (SEM) and presented in Figure 1. Sample (A) shows the porous network structure of silica aerogels. The particles size is about 68 nm. Sample (B) shows the porous network structure of eggshell and its particle size was about 300 nm. Sample (C) exhibits a porous network structure similar to sample (A) but the particles are smaller. It is obvious that sample (C) has the best network structure for the study of the absorption process.

3.1.2. FT-IR Spectrum of the adsorbents

In Figure 2a, the FT-IR investigation of silica aerogel nanocomposite is shown in comparison with pure silica aerogel. The peak obtained for SA samples appeared at 2982 cm^{-1} due to C–H group which cannot be observed in nanocomposite sample. The broad absorption band in the region at 3448cm^{-1} and the band at 1638 cm^{-1} on both graphs correspond to O–H stretching. The small peak in the SA sample at the region of 943 cm^{-1} is assignable to Si–OH bonds.

Peaks at 1048cm^{-1} and 840cm^{-1} also correspond to the Si–O–Si stretching on both graphs. It should be notified that the peaks generally seem wider in the absence of $CaCO_3$. This indicates that the presence of Ca^{2+} effects on the behavior of the surface Si–OH Monfared groups [27]. These FT-IR results suggest that the Ca^{2+} atoms are not covalently bonded to silicon in the silica aerogel network. The proposed mechanism for the combination of silica aerogel with $CaCO_3$ of eggshell is presented in Figure 3. After adsorption process, the FT-IR spectrum of adsorbents can be seen from Figure 2b. On both graphs, the peaks at around 3200 and 770cm^{-1} are related to the stretching and bending bonds of C=C–H in aromatic ring, respectively.

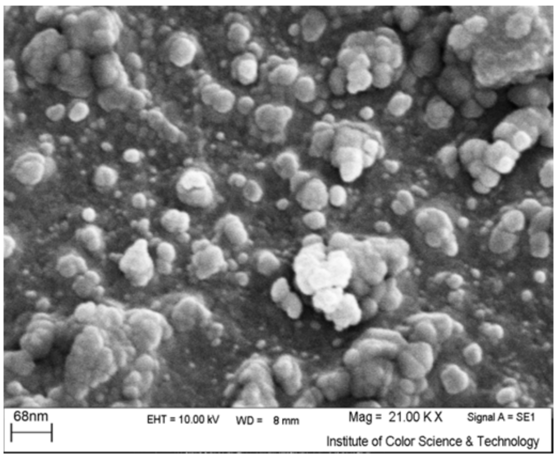

(A)

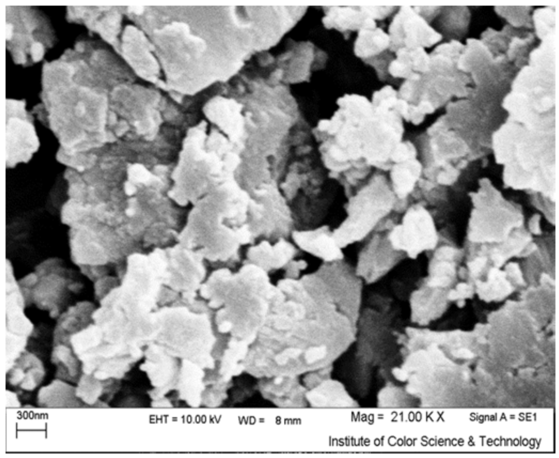

(B)

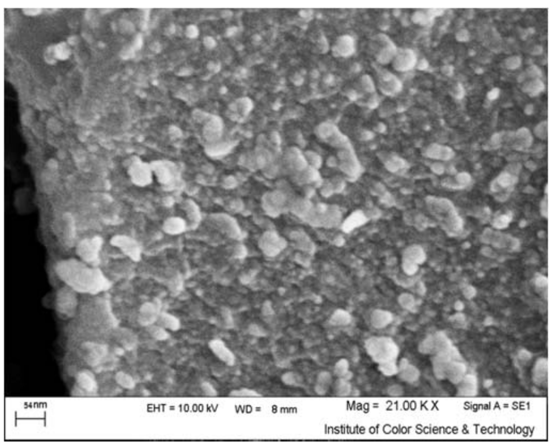

(C)

Figure 1: The SEM images of samples (A): silica aerogel (B), eggshell and nanocomposite (C).

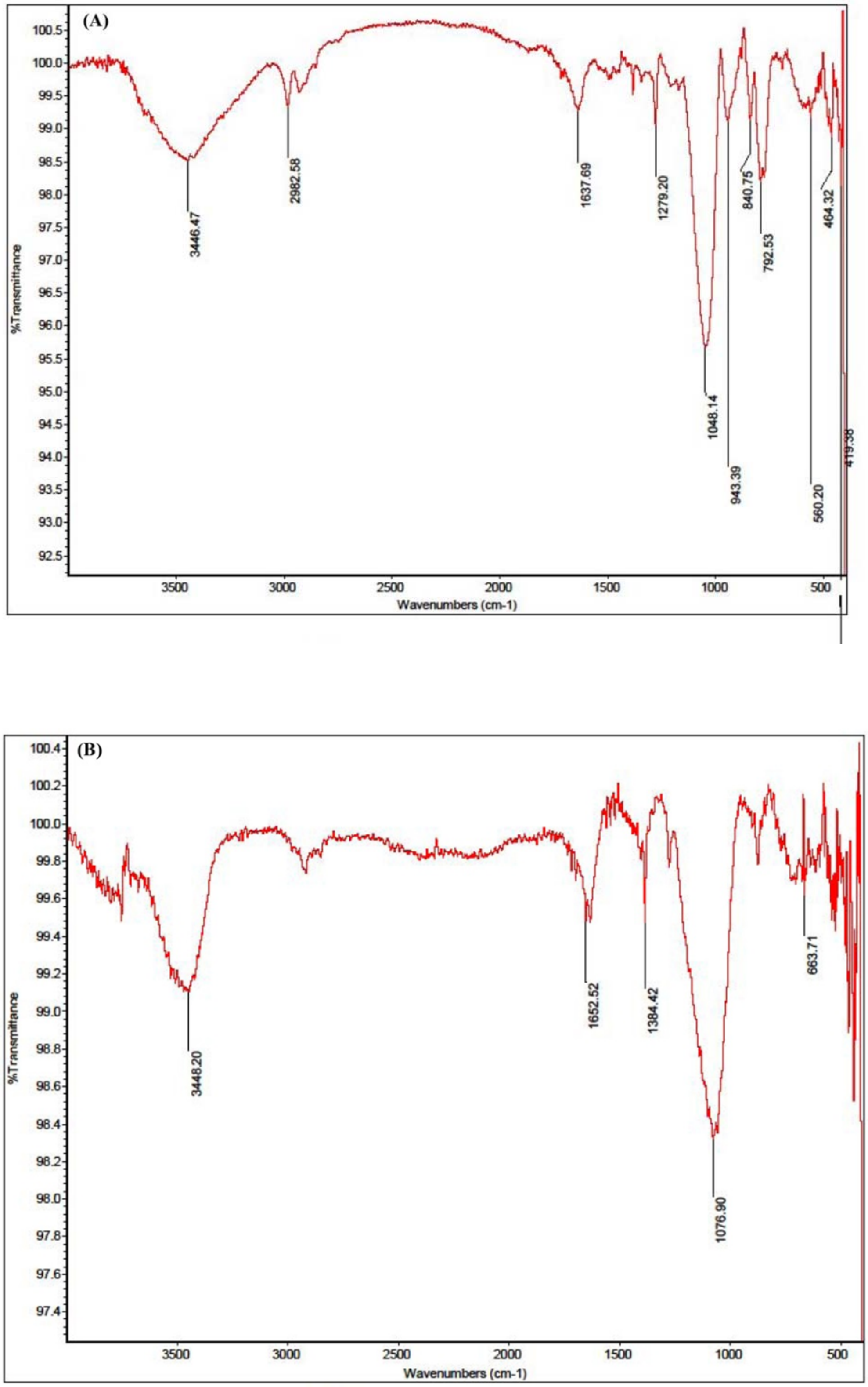

Figure 2a: FT-IR absorption spectra of silica aerogel (A)and nanocomposite silica aerogel-egg shell (B) before adsorption process.

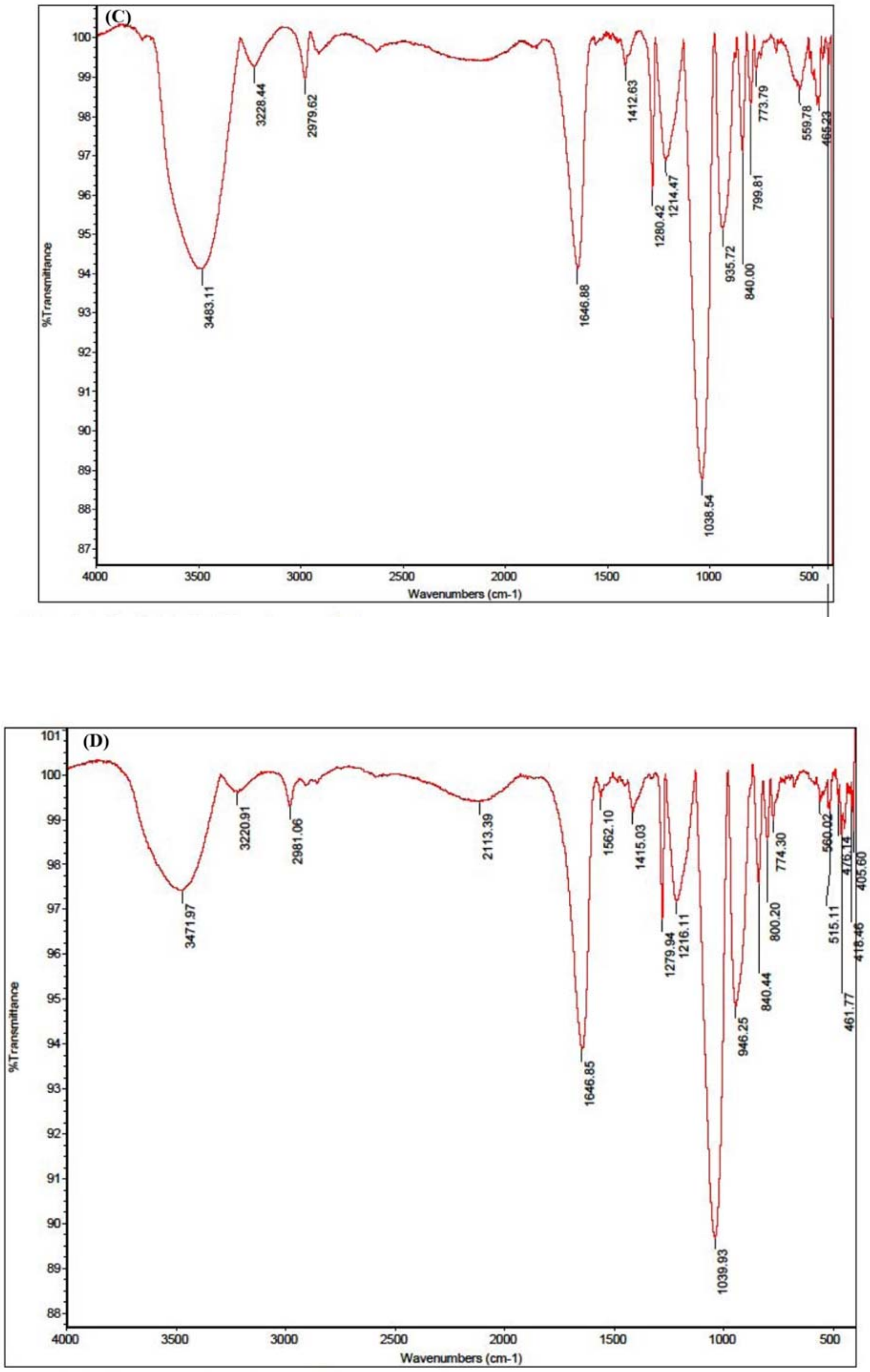

Figure 2b: FT-IR absorption spectra of silica aerogel (C) and nanocomposite silica aerogel-egg shell (D) after adsorption process.

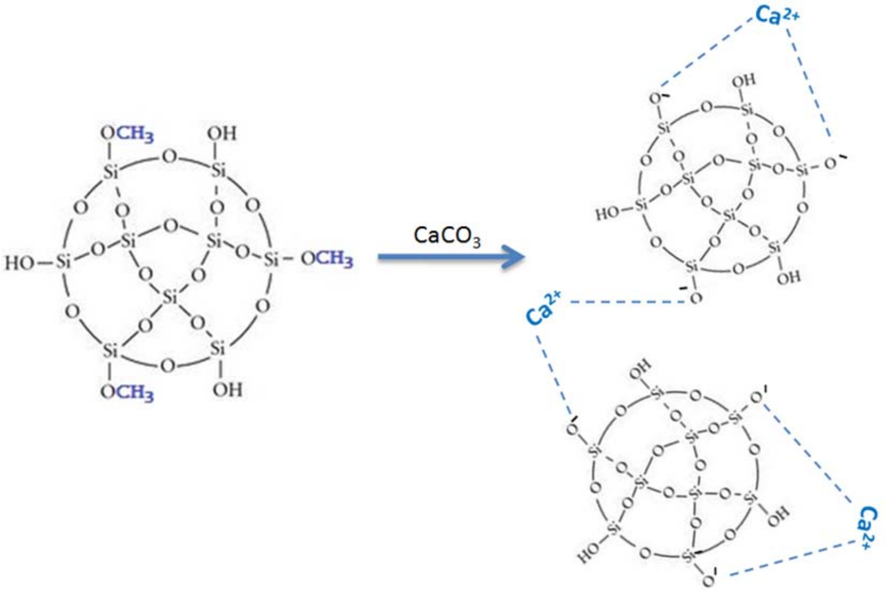

Figure 3: The proposed mechanism for the combination of silica aerogel with $CaCO_3$.

3.2. Effect of pH

The pH of the solution plays an important role in adsorption process as the creating positive or negative charge on the adsorbent surface [27, 28]. The experiments were carried out with the pH of 4–13, and its effect on the adsorption of dye ions by the three adsorbents (silica aerogel, eggshell and composite) is shown in Figure 4. The results show that the adsorption capacity of the adsorbents was increased at the pH of 12 for silica aerogel and eggshell and at pH of 8 for nanocomposite. At low pH values, the contest between ions of dey and protons resulted in weak adsorption of dye by silica aerogel and eggshell. More adsorption of dye took place at pH>10.The surface of the adsorbents is surrounded with dye ions in competition with OH ions in the alkaline environment. By increasing the pH value, the silica aerogel structure remained stable but the eggshell converted to the network structure of $Ca(OH)_2$. So the dye ions easily trapped by the adsorbents [29]. The adsorption capacity of nanocomposite reduced at pH of 10 because its structure was destroyed at high pH. However, the optimum pH for nanocomposite was considered in the ranges of 6 to 10.

3.3. The effect of initial concentration

Figure 5 indicates the effect of initial dye concentration on the adsorption capacity of three adsorbents. The increase of initial concentration of dye ions in the range of 5 to 50 mg/L causes the reduction of the removal yield. At low initial concentration, enough adsorption sites are available for adsorption. In other words, the available sites of adsorbents reduce at higher concentrations of the adsorbate [28].

3.4. The effect of adsorbent dose

To investigate the effect of different adsorbent dose for removal of BV16, several values of adsorbents were used in the range of 2-6g/L. The results in Figure 6 show the increasing of BV16 removal percentage by increasing the dose of adsorbent from 2 to 5g/L and was stabilized at a greater amount. This phenomenon is attributed to an increase in the number of adsorption site's availability and larger surface area of adsorbents versus constant rate of pollutant concentration [30].

3.5. The effect of contact time

The contact time was evaluated from the range of 30 to 210 min. Results in Figure 7 shows that the removal value of BV16 dye increases by increasing the contact time from 30 to 90 min. After 90 min, the amount of dye removal from the solution is slightly increased. The results can be attributed to the reduction of the amount of dye interferes with active sites on the adsorbents surface [13].

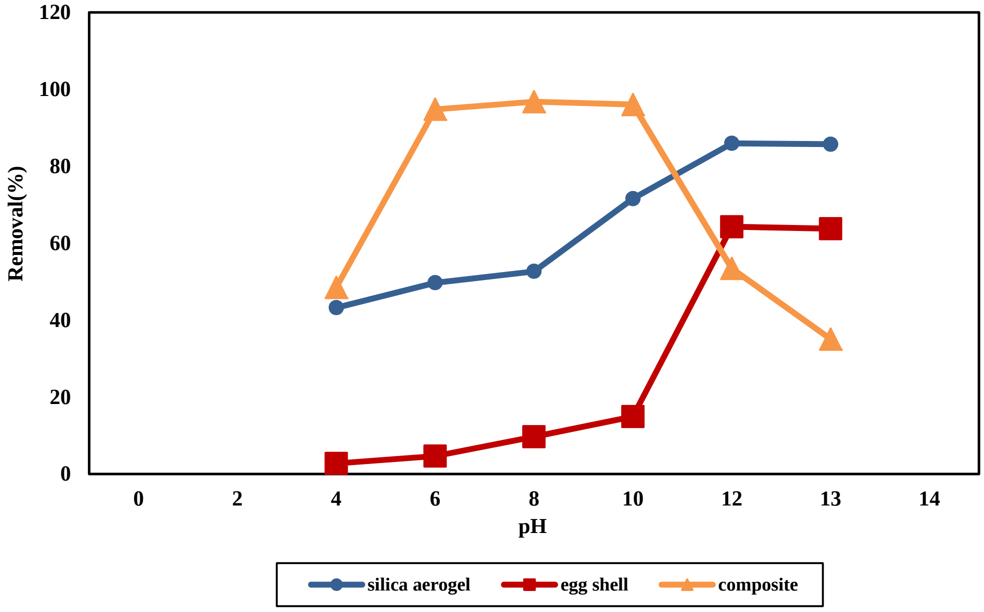

Figure 4: Removal percentage of BV16 ions at different pH values. Conditions: 0.1 g adsorbent, 20 ml of 10 mg/L of cadmium ions, contact time of 3h.

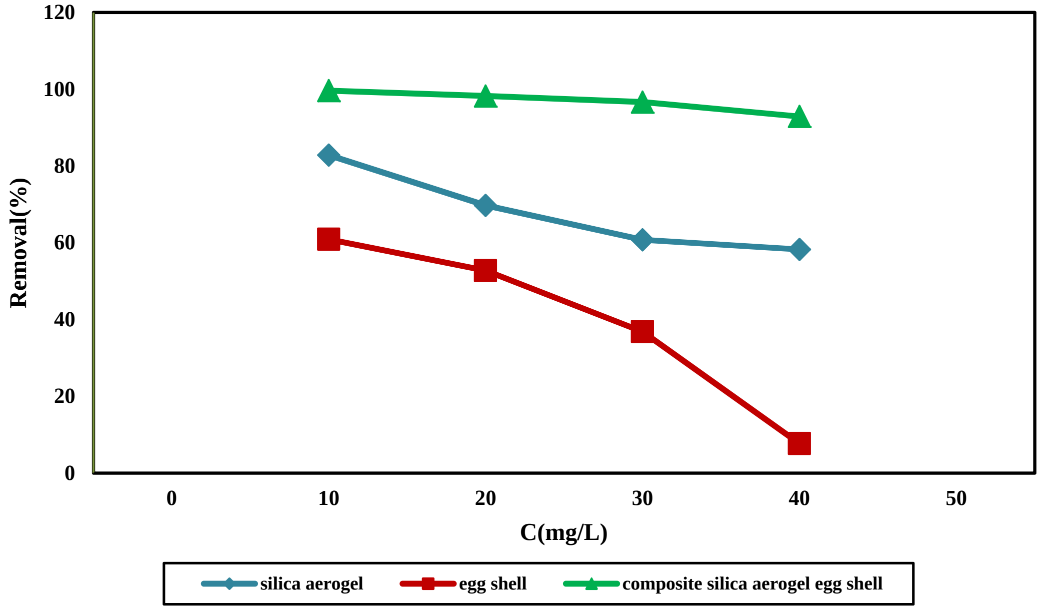

Figure 5: Effect of initial concentration on the removal yield of BV16; contact time = 3 h; adsorbent dose = 0.1, pH = 12 for silica aerogel and egg shell and 8 for nanocomposite.

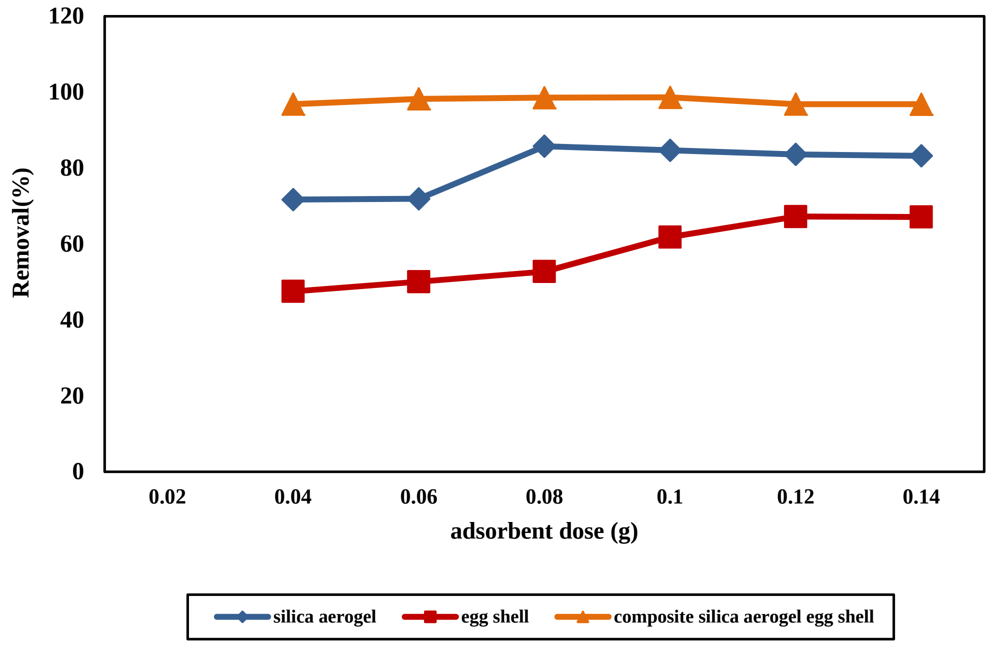

Figure 6: Effect of adsorbent dose on the removal yield of BV16; initial concentration=10mg/L; contact time=3h; pH=12 for silica aerogel and egg shell and 8 for nanocomposite.

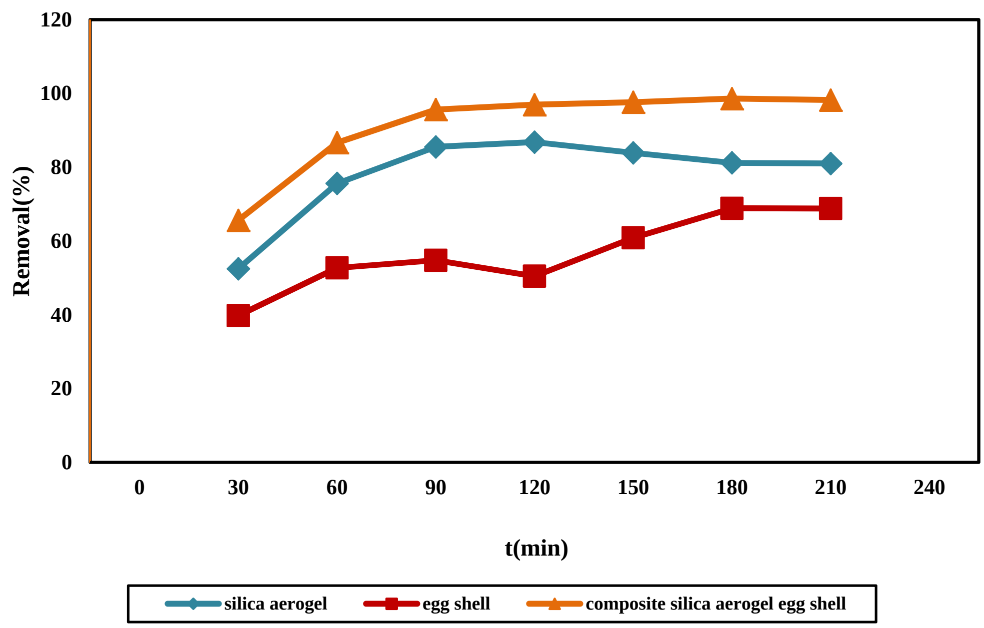

Figure 7: The effect of contact time on the removal yield of BV16; initial concentration=10mg/L; contact time=3h; pH=12 for silica aerogel and egg shell and 8 for nanocomposite**.**

3.6. The effect of temperature on adsorption

In order to appraise the influence of temperature on dye adsorption, the experiments were carried out at 25–65°C. From Figure 8 it can be deduced that the removal percent was decreased at temperatures higher than 35°C. In this case, the severe molecular movement leads to the release of dye as far as temperature is increased from 35 to 65°C [31].

3.7. Adsorption isotherms

Equilibrium isotherms are examined for the design of any adsorption process. Adsorption isotherm study is performed with the comparative adsorption of BV16 on three adsorbents at different temperatures (25, 35, 45 and 65°C). The adsorption isotherms can be studied by two models: Langmuir and Freundlich [32].

3.7.1 Langmuir Isotherm

The Langmuir adsorption model assumes monolayer adsorption on a homogeneous adsorbent, where all the sorption sites are indicative interaction with the adsorbed ion. There is no interaction between the adsorbed ions and sorption sites. The homogeneous Langmuir adsorption isotherm model is demonstrated by the following equation [32].

$$q_e=(q_{max}\ K_L\ C_e)/(1+K_L\ C_e) \quad (3)$$

where qe is the adsorbed amount of the dye at equilibrium ($mol.g^{-1}$), Ce is the equilibrium concentration of the dye in solution ($mol.dm^{-3}$), q_{max} is the maximum adsorption capacity ($mol.g^{-1}$) and K_L is the constant related to the free energy of adsorption ($dm^3.mol^{-1}$). These constants can be determined from the linear plot of C_e/q_e versus C_e (Figure 9).

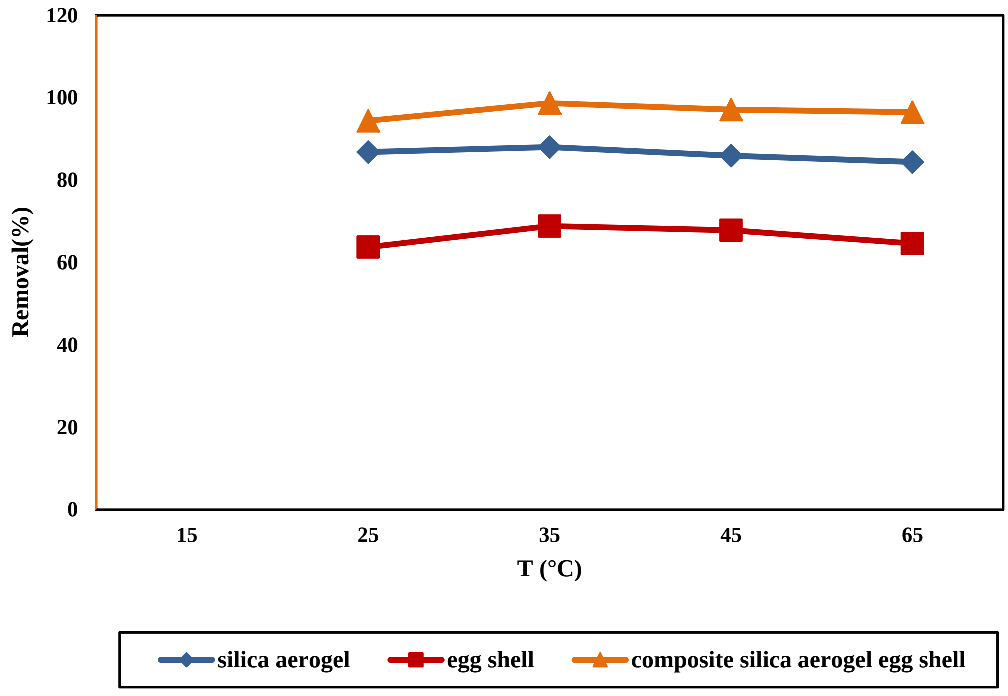

Figure 8: Effect of temperature on the removal yield of BV16; initial concentration=10 mg/L; contact time=3h; pH=12 for silica aerogel and egg shell and 8 for nanocomposite.

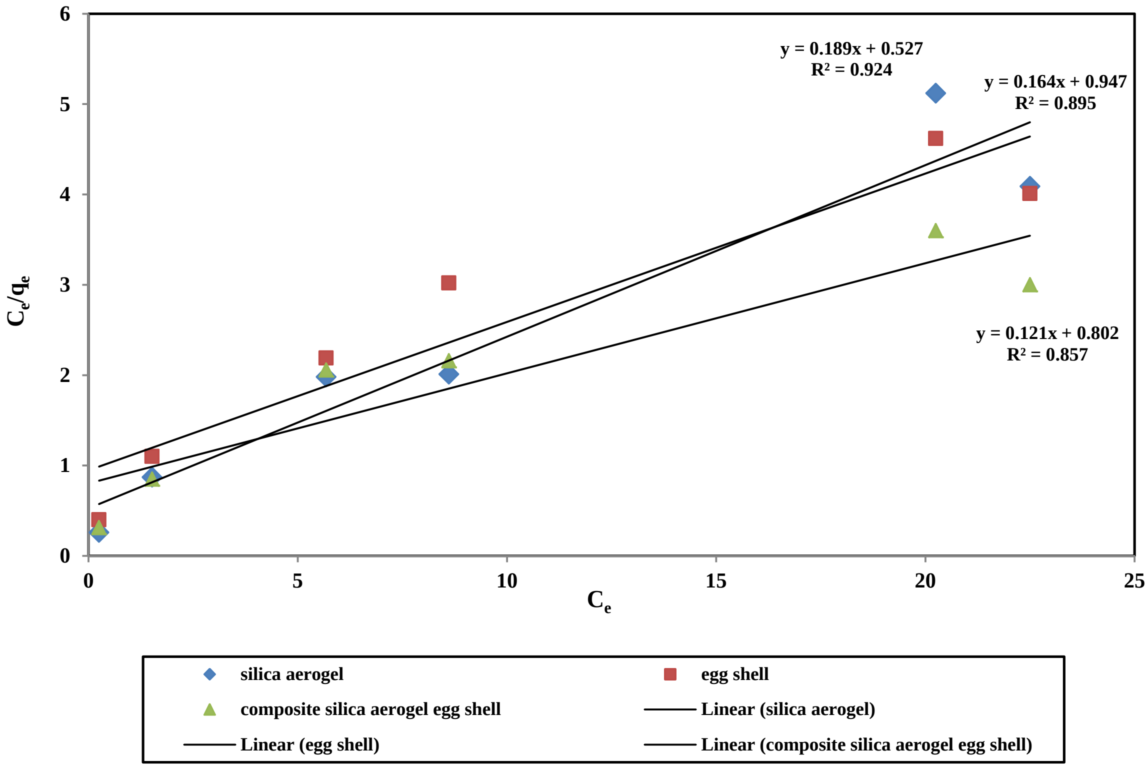

Figure 9: Langmuir plot showing the linear dependencies of C_e/q_e on C_e.

3.7.2 Freundlich Isotherm

The Freundlich Isotherm is a model investigating heterogeneous adsorption on the adsorbent surface. The Freundlich isotherm is expressed by equation (4) [32].

$$q_e = K_F\, C_e^{1/n} \quad (4)$$

Where K_F is the Freundlich constant ($L.mg^{-1}$), and n is the adsorption intensity. The linear graph of Freundlich isotherm models of BV16 adsorption was depicted in Figure 10. The slope and intercept are obtained from the plot of Log q_e against Log C_e. The adsorption isotherm results for the BV16 dye were matched with Freundlich isotherms, which were determined by the correlation coefficients (R_2).

3.8. Kinetic study

The effective factors on the reaction rates for the adsorption of BV16 on adsorbents were studied by adsorption kinetic experiments. Adsorption kinetics also describes how fast or slow the chemical reaction occurs. Two kinetic models (i.e. pseudo-first order and pseudo-second-order models) were tested with suitable adsorption kinetics data [33].

3.8.1 Pseudo-first-order model

The pseudo-first order rate explanation is generally proposed by equation (5).

$$\ln (q_e - q_t) = \ln q_e - k_1 t \quad (5)$$

where k_1 is the pseudo-first-order rate constant (min^{-1}), q_e and qt are the amount of dye adsorbed at equilibrium and time t ($mol.g^{-1}$), respectively. The plot of ln (q_e- q_t) versus t as shown in Figure 11 gave the slope k_1 and the intercept lnq_e.

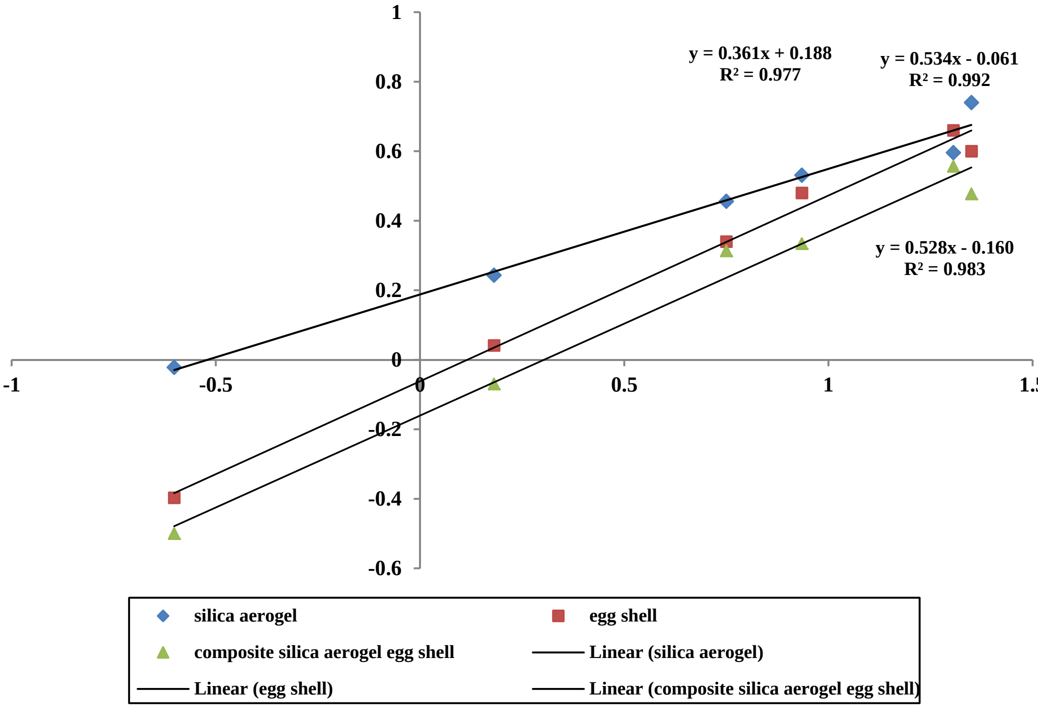

Figure10: Freundlich plot showing the linear dependences of log q_e on log C_e.

3.8.2 Pseudo-second-order model

The pseudo-second-order model is expressed by the following equation:

$$t/q_t = 1/\ k_2 q_e^2 + 1/\ q_e\ t \qquad (6)$$

Where k_2 is the rate constant of pseudo-second-order adsorption mechanism ($g.mol^{-1}.min^{-1}$). As given in Figure 12, the plot of t/q_t versus t shows a linear relevance, according to which the q_e and k_2 are calculated. The kinetic adsorption results were calculated using Eqs. (5) and (6) as shown in Table 2. It implies that BV16 adsorption is well explained by the pseudo second order kinetic model.

3.8. Desorption studies

Desorption studies help to explain the mechanism and recovery of the adsorbent. The adsorption of dye was investigated at different pH values 4, 12. The percent of dye desorption was 81.8% at pH=4 for BV16 dye. The percent of dye desorption was decreased with increasing pH. A negatively charged site on the adsorbent prevents desorption of dye captions. At pH 4, significantly high electrostatic repulsion exists between the positive charged surface of the adsorbent and cationic dye [34]. For desorption experiment, the adsorbents were washed with deionized water. The desorption of BV16 was then performed by putting the silica aerogel-eggshell nanoparticles into methanol solution containing 0–5% acetic acid [35].

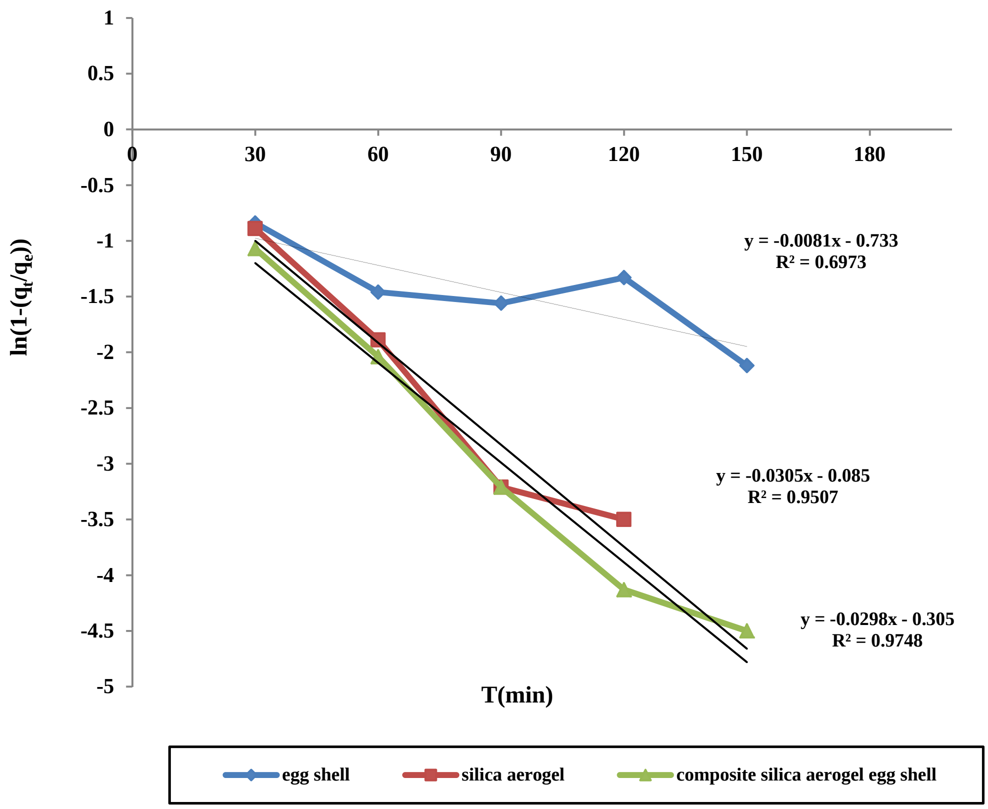

Figure 11: Pseudo-first order plot of BV16 adsorption.

Table 2: Kinetic parameters for pseudo-first order and pseudo-second order models of BV16 adsorption using three adsorbents.

kinetic models	Parameters	Eggshell	Aerogel	Composite
Pseudo-first order model	K_1	0.008	0.03	0.029
	$q_{e\ cal}$	1.076	1.08	1.35
	$q_{e\ exp}$	1.37	1.78	1.97
	R_2	0.697	0.95	0.974
Pseudo-second order model	K_2	0.02	0.036	0.029
	$q_{e\ cal}$	1.51	1.86	2.16
	$q_{e\ exp}$	1.37	1.78	1.97
	R_2	0.938	0.977	0.997

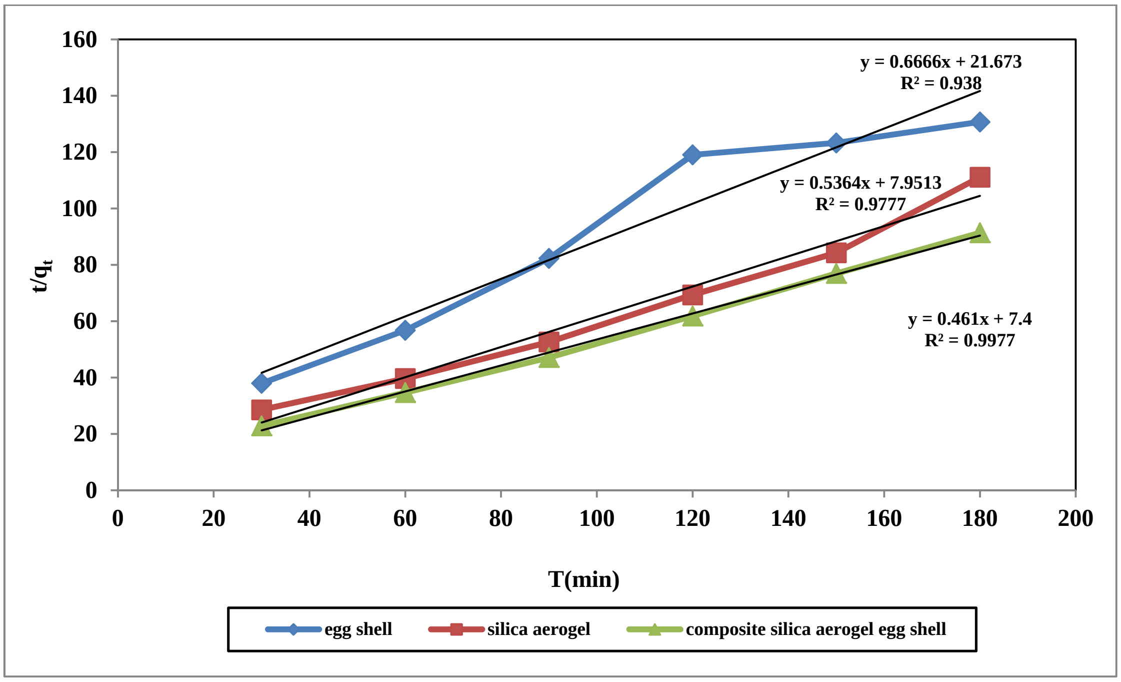

Figure 12: Pseudo-second order plot of BV16 adsorption.

4. Conclusions

The silica aerogel- eggshell nanocomposite has been carefully synthesized at room temperature by sol-gel procedure. Three adsorbents named silica aerogel, eggshell and nanocomposite silica aerogel-eggshell have been tested for the removal of basic violet 16 from aqueous solutions in batch system. The structure of adsorbents was characterized by Fourier transform infrared spectra (FT-IR) and scanning electron microscope (SEM). The BV16 adsorption capacity was found to increase with increasing pH, contact time, adsorbent dose and temperature. The suitable isotherms were chosen according to Langmuir and Freundlich models. The data obtained from the kinetic study determined that the adsorption of BV16 follows pseudo-second order rate equation. Hence, the rate-limiting step can be chemisorption. The desorption experiments confirmed that the nanocomposite can be used again without any reduction in dye removal yield.

5. References

1. B. S. Ratna, Pollution due to synthetic dyes toxicity & carcinogenicity studies and remediation, *Int J Eng Sci*, 3 (2012), 940-955.
2. A. Z. M. Badruddoza, Si. Si. Hazel Goh, K. Hidajat, M. S. Uddin, Synthesis of carboxymethylcyclodextrin conjugated magnetic nano-adsorbent for removal of methylene blue, *Colloids Surf.*, 367(2010), 85-95.
3. Z. Carmen, S. Daniela, Textile Organic Dyes – Characteristics, Polluting Effects and Separation/Elimination Procedures from Industrial Effluents – A Critical Overview, Environmental and Analytical Update, Pub: InTech, 2012, 55-86
4. A. Pirkarami, M. E. Olya, N. Yousefi Limaee, Decolorization of azo dyes by photo electro adsorption process using polyaniline coated electrode, *Prog. Org. Coat.*, 76(2013), 682- 688.
5. Z. Rahmani, M. Kermani, M. Gholami, A.

Jonidi Jafari, N.M. Mahmoodi, Effectiveness of photochemical and sonochemical processes in degradation of Basic Violet 16 (BV16) dye from aqueous solutions. *Iran. J. Environ. Health. Sci. Eng.,* (2012), 1-7.

6. B. Xin, O. Huang, S. Chen, X. Tang, High-purity Nano Particles ZnS Production by a Simple Coupling Reaction Process of Biological Reduction and Chemical Precipitation Mediated with EDTA, *Biotechnol. Prog.,* 24(2008), 1171-1177.
7. M. Caetano, C. Valderrama, A. Farran, J. L. Cortina, Phenol removal from aqueous solution by adsorption and ion exchange mechanisms onto polymeric resins, *J. Colloid Interface Sci.*, 338(2009) 402-409.
8. M. Turek, P. Dydo, J. Trojanowska, A. Campen, Adsorption/co-precipitation-reverse osmosis system for boron removal, *Desalination*, 205(2007), 192-199.
9. K. Ayoub, S. Nelieu, E. D. Hullebusch, J. Labanowski, I. Schmitz-Afonso, A. Bermond, M. Cassir, Electro-Fenton removal of TNT: Evidences of the electro-chemical reduction Contribution, *Appl. Catal., B*, 104(2011), 169-176.
10. V. Kumar Gupta, R. Jain, S. Varshney, V. Kumar Saini, Removal of Reactofix Navy Blue 2 GFN from aqueous solutions using adsorption techniques, *J. Colloid Interface Sci.*, 307(2007), 326-332.
11. S. Štandeke, V. Veronovski, Z. Novak, Ž. Knez, Silica aerogels modified with mercapto functional groups used for Cu(II) and Hg(II) removal from aqueous solutions, *Desalination,* 269(2011), 223-230.
12. S. Buthelezi, A. Olaniran, B. Pillay, Textile Dye Removal from Wastewater Effluents Using Bioflocculants Produced by Indigenous Bacterial Isolates, *Molecules,* 17(2012), 14260-14274.
13. M. T. Ghaneian, M. Momtaz, M. Dehvari, An Investigation of the Efficacy of Cuttlefish Bone Powder in the Removal of Reactive Blue 19 Dye from Aqueous Solutions: Equilibrium and Isotherm Studies, *J. Taiwan Inst. Chem. Eng.,* 3(2012), 68-78.
14. L. H. Wang, C. I. Li, Equilibrium study on chromium (III) ion removal by adsorption onto rice hull ash, *J. Taiwan Inst. Chem. Eng.,* 40(2009), 110-112.
15. A. R. Dincer, Y. Gu¨nes, N, Karakaya, E. Gu¨nes, Comparison of activated carbon and bottom ash for removal of reactive dye from aqueous solution. *Bioresour. Technol.,* 98(2007), 834-839.
16. H. Liu, W. Sha, A. T. Cooper, M. Fan, Preparation and characterization of a novel silica aerogel as adsorbent for toxic organic compounds. *Colloids Surf.*, 347(2009), 38-44.
17. Y. E. Guanghua , Zh. Kake, Zh. Xinggui, C. Marc-Olivier, Y. Weikang, Optimizing spatial pore-size and porosity distributions of adsorbents for enhanced adsorption and desorption performance, *Chem. Eng. Sci.,* 132 (2015), 108-117.
18. R. P. Patel, N. S. Purohit, A. M. Suthar, An Overview of Silica Aerogels. *Int J ChemTech Res*, (2009), 1052-1057.
19. K. Sinkó, Influence of Chemical Conditions on the Nanoporous Structure of Silicate Aerogels, *Materials*, 3(2010), 704-740.
20. J. P Nayak, J. Bera, Preparation of Silica Aerogel by Ambient Pressure Drying Process using Rice Husk Ash as Raw Material. Trans. *Ind. Ceram. Soc.*, 68(2009), 1-4.
21. G. Krithiga, T. Sastry, Preparation and characterization of a novel bone graft composite containing bone ash and eggshell powder, *Bull. Mater. Sci.* 34(2011), 177-181.
22. C. Shen, Y.Wang, J. Xu, Y. Lu, G. LuoG, Preparation and ion exchange properties of egg-shell glass beads with different surface morphologies, *Particuology,* 10(2012), 317-326.
23. V. Hernández-Montoy, L. A. Ramírez-Montoya, A. Bonilla-Petriciolet, M.A. Montes-Morán M A, Optimizing the removal of fluoride from water using new carbons obtained by modification of nut shell with a calcium solution from eggshell, *Biochem. Eng. J.,* 62(2012) 1-7.
24. M. H. Givianrad, M. Rabani, M. Saber-Tehrani, P. Aberoomand-Azar, M. Hosseini Sabzevari, Preparation and characterization of nanocomposite, silica aerogel, activated carbon and its adsorption properties for Cd (II) ions from aqueous solution, *J. Saudi Chem. Soc.,*17(2013), 329-335.

25. M. Arami, N. Yousefi Limaee, N. M. Niyaz Mohammad Mahmoodi, Investigation on the adsorption capability of eggshell membrane towards model textile dyes, *Chemosphere*, 65 (2006), 1999–2008.
26. A. Soleimani Dorcheh, M. H. Abbasi, Silica aerogel; synthesis, properties and characterization, *J. Mater. Process. Technol.,* 199(2008), 10-26.
27. S. Masoudian, H. Hosseini Monfared, Silica aerogel–iron oxide nano-composites: recoverable catalysts for the oxidation of alcohols with hydrogen peroxide, *Transition Met. Chem*, 36(2011), 521-530.
28. R. H. Pouretedal, M. Kazemi, Characterization of modified silica aerogel using odium silicate precursor and its application as adsorbent of Cu^{2+}, Cd^{2+}, and Pb^{2+} ions, *Int. J. Ind. Chem*., 20(2012), 1-8.
29. M. Pettinato, S. Chakraborty, A. Hassan, V. Calabro, Eggshell: A green adsorbent for heavy metal removal in an MBR system. *Ecotoxicol. Environ. Saf.,* 121(2015), 57-62.
30. K. Santhy, P. Selvapathy, Removal of reactive dyes from wastewater by adsorption on coir pith activated carbon, *Bioresour. Technol.,* 97(2006), 1329-1336.
31. . M. F. Elkady, A. M. Ibrahim, M. M. Abd El-Latif, Assessment of the adsorption kinetics, equilibrium and thermodynamic for the potential removal of reactive red dye using eggshell biocomposite beads, *Desalination*, 278 (2011), 412-423.
32. K. Bellir, I. Sadok Bouziane, Z. Boutamine, M. Bencheikh Lehocine, A. H. Meniai, Sorption Study of a Basic “Gentian Violet” from Aqueous Solutions Using Activated Bentonite, *Energy Procedia*, 18(2012) 924-933.
33. A. Malviya, D. Kaur, Removal of Toxic Azo Dyes from Wastewater using Bottom Ash - Equilibrium Isothermal Modeling, *Orient. J. Chem.,* (2012), 955-961.
34. M. Mohamad Rasool, M. Ali Khan, S. Hosseini, A. Luqman Chuah, S. Y. Choong, Adsorption/desorption of cationic dye on surfactant modified mesoporous carbon coated monolith: Equilibrium, kinetic and thermodynamic studies, *J. Ind. Eng. Chem*., 21(2015), 369-377.
35. S. Y. Mak, D. H. Chen, Fast adsorption of methylene blue on polyacrylicacid-bound iron oxide magnetic nanoparticles, *Dyes Pigment,* 61(2004), 93-98.